New insight on crystal and spot development in hard and extra hard cheeses: association of spots with incomplete aggregation of curd granules

Journal:	*Journal of Dairy Science*
Manuscript ID	JDS-16-11050.R1
Article Type:	Research
Date Submitted by the Author:	n/a
Complete List of Authors:	D'Incecco, Paolo; University of Milan, Department of Food, Environmental and Nutritional Sciences Limbo, Sara; University of Milan, Department of Food Environmental and Nutritional Sciences Faoro, Franco; University of Milan, Department of Agricultural and Environmental Sciences - Production, Landscape, Agroenergy Hogenboom, John; University of Milan, Department of Food Environmental and Nutritional Sciences Rosi, Veronica; University of Milan, Department of Food Environmental and Nutritional Sciences Morandi, Stefano; National Research Council , ISPA Pellegrino, Luisa; University of Milan, Department of Food Environmental and Nutritional Sciences
Key Words:	hard and extra hard cheeses, cheese ultrastructure, calcium phosphate crystal, free amino acids

INTERPRETATIVE SUMMARY

New insight on crystal and spot development in hard and extra hard cheeses: association of spots with incomplete aggregation of curd granules

D'Incecco

The study was carried out with a multidisciplinary approach, using techniques such as confocal, Raman and electron microscopy, to shed light on the phenomenon of speck and spot blowing in hard cheese. The obtained information on structure and chemical composition of these particles, allowed us to formulate an original theory for their genesis. Furthermore, these results provide useful information to be applied in cheese making technology in order to contain the incidence of the speck and spot phenomenon.

RUNNING HEAD: CRYSTALS AND SPOTS IN HARD AND EXTRA HARD CHEESES

New insight on crystal and spot development in hard and extra hard cheeses: association of spots with incomplete aggregation of curd granules

P. D'Incecco,*[1] S. Limbo,* F. Faoro,[†] J. Hogenboom,* V. Rosi,* S. Morandi,[‡] L. Pellegrino*

* Department of Food Environmental and Nutritional Sciences, State University of Milan, 20133 Milan, Italy.

[†] Department of Agricultural and Environmental Sciences - Production, Landscape, Agroenergy, State University of Milan, 20133 Milan, Italy.

[‡] Institute of Sciences of Food Production–Italian National Research Council, 20133 Milan, Italy.

[1]Corresponding author: P. D'Incecco

Department of Food, Environmental and Nutritional Sciences, University of Milan, Via Celoria 2, 20133 Milan, Italy

Telephone: (+39) 0250316679

Fax: (+39) 0250316672

E-mail: paolo.dincecco@unimi.it

ABSTRACT

Chemical composition and structure of different types of macro- (specks, spots) and micro particles (microcrystals) present in hard and extra hard cheeses were investigated. Light microscopy revealed that the small, hard specks had the structure of crystalline tyrosine, as confirmed by amino acid analysis. Spots showed a complex structure, including several curd granules, cavities, and microcrystals, and were delimited by a dense protein layer. Spots contained less moisture and ash than the adjacent cheese area, and more protein, including significantly higher contents of valine, methionine, isoleucine, leucine, tyrosine and phenylalanine. Microcrystals were observed by light and electron microscopy and analysed by confocal micro Raman. Among others, calcium phosphate crystals appeared to consist of a central star-shaped structure immersed in a matrix of free fatty acids besides leucine and phenylalanine, in free form or in small peptides. A hypothetical mechanism for the formation of these structures has been formulated.

Keywords: hard and extra hard cheeses, cheese ultrastructure, calcium phosphate crystal, free amino acids, electron microscopy

INTRODUCTION

Hard and Extra-Hard are attributes used to define cheeses having a firm and brittle body texture (Codex Alimentarius, 1978). Hard and extra-hard cheeses share low moisture content, close structure, and a long ripening period. During ripening, many chemical, biochemical and microbiological phenomena take place. The biochemical changes are very important for the development of the flavour and texture of these cheeses and are characteristic of the different varieties. Proteolysis is the most relevant among the biochemical phenomena due to its complexity and final impact on the cheese taste. In fact, casein breakdown progressively brings to large and medium peptides, then to small peptides and free amino acids (FAA). Since FAA are rather stable, they tend to accumulate with the ripening time and may reach up to 20-24% on cheese protein basis in 10-12 months old extra-hard cheeses (Masotti et al., 2010). Proteinases and peptidases that catalyse proteolysis in cheese originate from different sources, namely milk, rennet, starter and non-starter lactic acid bacteria (LAB). LAB have complex enzyme patterns that release peptides and amino acids from the proteins into the cheese environment to satisfy their own nutritional requirements (Gatti et al., 2014). After vat processing, the loss of water, diffusion of salt, and formation of soluble molecules, such as FAA and lactate, are factors concurring to the increase of solute concentration and concomitant decrease of water activity (a_w) in cheese throughout the whole ripening period. Beside these main events, minor changes contribute to lower the water activity in cheese, like changes in water binding by new carboxylic and amino groups formed on protein hydrolysis (McSweeney, 2004). The moisture content and a_w are strongly correlated in cheese throughout ripening (Marcos, 1993).

The increasing solute (salt, ions, FAA) concentration in cheese water phase may give rise to aggregation and crystallization phenomena that result in different types of structures observed by some authors in the interior and on the surface of different cheese varieties (Bianchi et al., 1974; Agarwal et al., 2006; Tansman et al., 2015). Although earliest studies date back to the 1900s

(Babcock et al., 1903; Tuckey et al., 1938), a clear and unambiguous characterization of these structures has not been achieved yet. Moreover, an univocal association between the terminology (e.g. crystals, specks, dots, granules, spots, pearls) and the appearance of these structures is still lacking.

In long ripened extra-hard cheeses, having a thick dry rind, these structures develop inside the cheese becoming visible when the wheel is cut. Typically, two different types of structures visible to the naked eye can be observed, referred to as specks and spots in this article. Specks look bright white and firmer against the cheese matrix, and are usually smaller than 2-3 mm. Consumers (cheese lovers) appreciate the crispness of the specks while chewing the cheese and their contribution to the overall cheese taste. Previous studies about specks reported them to contain clusters of tyrosine, cysteine as well as other FAA, calcium lactate and magnesium (Shock et al. 1948) or tyrosine and phenylalanine (Giolitti and Mascherpa, 1970). More recently, Bottazzi et al., (1994) and Tansman et al., (2015) converged on identifying them as tyrosine crystals in extra hard cheeses.

Spots are spherical and paler than the cheese, and can grow up to 4-5 mm. They appear to be amorphous and firmer with respect to the surrounding cheese matrix, and become visible after 10-12 months of ripening. Spots can become so numerous and flashy that may influence the visual appeal of the cheese. Spots have been very little studied, moreover without achieving consistent results (Giolitti and Mascherpa, 1970; Bianchi et al., 1974; Tansman et al., 2015).

Besides specks and spots, extra-hard cheeses contain microscopic crystals, mostly investigated in Cheddar cheese. However, some authors generically referred to crystals, without distinguishing between the microscopic ones and those visible to the naked eye (Kalab, 1980; Bottazzi et al., 1982; Washam et al., 1985; Bottazzi et al., 1994).

The aim of the present work was to shed light on the nature and origin of specks, spots and microscopic crystals in extra-hard cheeses by a multidisciplinary approach. Due to the effectiveness in cheese structure studies (Ong et al., 2010; Schrader et al., 2012; D'Incecco et al., 2015), various

microscopy techniques and different dyes (light and fluorescence, confocal, confocal micro Raman and transmission electron microscopy) were used in combination with chemical data to achieve an unambiguous characterization of these particles in cheese. Our ultimate goal was to formulate an hypothesis on the origin of these structures as they appear in hard and extra-hard cheeses. This knowledge will contribute useful information to understanding the bioavailability of selected minerals and nutrients in cheese. Furthermore, this knowledge could provide insights into the nature of these structures that might lead to new manufacturing strategies to control the formation of spots in commercial cheeses.

MATERIALS AND METHODS

Cheese samples and collection of specks and spots. Eleven extra-hard cheeses, ripened for 18-20 months, were kindly provided by two dairies producing Grana Padano (7 cheeses) and Parmigiano-Reggiano (4 cheeses) respectively. Specks were harvested from the cheese using a pin, while spots were collected from the cheese using a spatula and then gently brushed to remove the cheese matrix on the surface. Specks and spots were separately collected from individual cheese samples in a sufficient amount (20-22 g) to conduct all the analyses. Equivalent cheese amount was taken from the portion (0.5-cm thick) immediately surrounding the single spot, as shown in Figure 1, as used as a term of reference. When necessary, a slice representative of the whole cheese was taken as well. Additional cheese portions were taken as required for microscopy investigations with various techniques. In particular, 20 spots of different size and taken from different cheeses were observed for their structural characterization.

Chemicals.

Glutaraldehyde, paraformaldehyde, cacodylate buffer, and osmium tetroxide were purchased from Agar Scientific (Stansted, UK). Toluidine blue, rhodamine and single amino acids were purchased from Sigma Aldrich (Milan, Italy). Ninhydrin was purchased from Biochrom Ltd (Cambridge, UK). Water purified with Milli-Q system (Millipore Corp., Bedford, MA) was used.

Composition analyses.

The ISO Standard methods for cheese were used to determine the content of protein (ISO 27871:2011), fat (ISO 1735:2004), ash (ISO 5545:2008) and moisture (ISO5534:2004), respectively. Content of calcium and phosphorus were determined by ICP-MS spectrometer (Agilent Technologies, Milan, Italy).

The pattern of FAA was determined on the various cheese portions (including pecks and spots) using the method described by Masotti et al. (2010). Briefly, the cheese portion was solubilized with sodium citrate, homogenized and deproteinized with sulphosalicilic acid. The extract was diluted (1:1) with lithium citrate buffer at pH 2.2, filtered and analysed by ion exchange chromatography. The chromatographic separation was carried out on a Biochrom 30+ (Biochrom Ltd, Cambridge, UK) amino acid analyser operated under the conditions provided by the manufacturer. These employ an eight-step elution program with lithium citrate buffers of increasing pH and ionic strength, post-column derivatisation with ninhydrin, and detection at 440 and 570 nm. The quantification was carried out using four-level calibration lines of the 21 amino acids in the range 0.75-22.5 mg/L and using norleucine (Sigma Aldrich) as an internal standard. Repeatability values of ISO Standard 13903:2005 were fulfilled.

Amino acid diffusion trial.

To confirm the different diffusivity of individual FAA within the cheese, 0.3 mL of an aqueous FAA solution having three times the concentration of the cheese water phase was injected into the core of a spot-free cheese portion (a disk of 10 g) using a microsyringe. The cheese portion was kept in a forced-ventilation thermostatic oven at 18 °C for 18 days and then sampled as described in the Results. The FAA pattern and the moisture content were determined in each sampled portion.

Light and Confocal Microscopy.

Specimens for light and fluorescence microscopy observations were thin sections obtained from resin-embedded cheese samples prepared as below described for transmission electron microscopy (TEM). Thin sections (4-5 per sample) were directly dried on the microscope slide, stained and subsequently washed. Two different staining were performed, (i) toluidine blue (1% in water, w/v)

for 5 min at room temperature, to visualize the overall protein structure by light microscopy, and (ii) rhodamine B (0.5% in water, w/v) for 5 min at room temperature. In the latter case, the sample was examined by a Hg lamp, with the following filters: excitation wavelength = 570 nm, emission wavelength = 590 nm. In addition a 5-cm cube of cheese was immersed in ninhydrin solution for 1 h and then cut with a blade until a thin section containing a spot was obtained. All samples were examined with an Olympus BX optical microscope (Tokyo, Japan) equipped with Nomarski interference contrast and QImaging Retiga camera (Surrey, BC, Canada). Specimens for confocal microscopy observations were cryo-sectioned by a CM1950 cryostat (Leica, Germany) and stained directly onto the microscope slide with fast green (0.1 % in water, w/v). Sections were examined with a Video confocal microscope, Nikon Vico (Tokyo, Japan).

Transmission Electron Microscopy.

Cubes of cheese (1 mm edge length) were fixed in a mixture (w/v) of glutaraldehyde 3% and paraformaldehyde 2% in cacodylate buffer for 2 h at 4 °C, then washed with cacodylate buffer for 1 h and post-fixed in osmium tetroxide (1% in water, w/v) for 2 h. After the dehydration in an ethanol series, the samples were embedded in London Resin White ™ resin and cured at 60 °C for 24 h. Ultrathin sections (50 to 60 nm thick) were stained with uranyl acetate and lead citrate and examined with a Philips E208 transmission electron microscope (Aachen, Germany).

Confocal Micro Raman.

The Raman spectral data were collected in the range from 3200 to 200/cm Raman shift using a confocal DXR Raman Microscope (Thermo Scientific, Waltham, MA, USA). An Olympus 50X objective (numerical aperture 0.75) with a 50 µm confocal pinhole was used to collect the Raman signal directly from a flat area of the sample (cut using a sharp knife) with a spatial resolution lower than 1 µm, without any preparation of the sample. A laser with an excitation wavelength of 780 nm with a low energy power (5-10 mW) to avoid overheating and a 400 lines/mm grating was used to record Raman spectra over the focalized area. A photobleaching time equal to 1 min was set up. For the specks, spectra were collected individually while for the microcrystals a selected area was

analysed collecting around 70 spectra over the entire surface, using 10 µm as the interval between positions. In particular, each sample was placed on an automated x,y mapping stage and Raman spectra were obtained at different points of the selected surface, by moving it under the microscope objective. Autofocus at each map point was applied. Omnic Atlµs software (Thermo Fisher Scientific, Madison, WI, USA) was used to obtain Raman spectra, perform spectrometer operations and process data. All spectra were corrected for background contributions and an automated subtraction of cosmic ray peaks was employed.

Statistical analysis

Statistical treatment of data was performed by means of SPSS Win 12.0 program (SPSS Inc., Chicago, IL, USA). Data were analysed by Student's t-test and one way Anova. A $P<0.05$ was assumed as significance limit.

RESULTS

Speck characterization. Attempts to obtain a section of specks or to embed them in resin failed because they were too hard and packed. In contrast, specks *in toto* could be directly observed by light microscopy after isolation by cheese and showed the characteristic structure of crystalline tyrosine (Figure 2). The FAA pattern (Figure 2) indicated that specks were indeed tyrosine crystals of > 95% purity. The peak of ammonia in the chromatogram derived from the elution buffers and thus was ignored in purity calculation. The Raman spectrum also confirmed the nature of the specks: the doublet Raman bands at 828 and 848/cm due to the Fermi resonance between ring fundamental and overtone were strongly evident, as was the ring-O stretching vibration located at 1263/cm (Culka et al., 2010). Also the highly resolved bands found in the finger print region (1614-250/cm) were associated to the signals collected for the solid and pure (98-99%) crystalline form of L-tyrosine (spectrum not shown).

Spot characterization.

Spot structure was firstly examined by light microscopy. A cheese portion was immersed in the protein-staining solution (ninhydrin) and then sectioned up to reveal a spot inside which appeared

surrounded by an highly dense layer (Figure 3, arrowhead) that impaired staining permeation inside. However, some stain could permeate through preferential micro pathways (junctions, indicated by arrows in Figure 3), making the structure visible. Thin sections of resin-embedded spots, stained with toluidine blue, gave more insight of the inner structure (Figure 4a). The spot appeared as made of several curd particles having clean-cut irregular shapes and size up to 0.5 mm. The darker lines, corresponding to the junctions among curd particles, were richer in protein than the particle body. Several openings, including a large hole collecting the junctions, were visible in the section (Figure 4b). Although the cheese around the spot showed the same composite structure (not shown), large cavities were observed only inside spots. With respect to the curd particles, the junctions appeared as thick protein strings almost free of fat (Figure 4c) and rich in microcrystals (arrows). Microcrystals were also observed in the cheese matrix outside the spot, as further discussed.

The ultrastructure of the spot, examined by TEM, proved to be remarkably different compared to that of the surrounding cheese (Figure 5). In particular, the interface between protein (Figure 5, in grey) and fat (in white) was more irregular and fringed by crystal-like particles (Figure 5a) in respect with the cheese surrounding the spot (Figure 5b).

The chemical composition of the spots was compared to that of the cheese portion just around them and to that of the whole cheese. Five different cheeses were individually analysed (Table 1). Spots proved to be significantly richer in protein ($p<0.00$) and poorer in moisture ($p<0.00$) and ash ($p<0.00$) with respect to the surrounding cheese portion, which did not differ from the whole cheese. Fat content was not different ($p<0.17$). The contents of both calcium and phosphorus were 10% lower in the spot than in the cheese, with a Ca/P molar ratio of 1 in both zones (not shown). The protein fraction was characterized by capillary zone electrophoresis as described in our previous work (Masotti et al., 2010). No difference could be evidenced, neither in casein nor in peptide patterns, between the spots and the rest of the cheese (not shown), indicating that the primary proteolysis had proceeded to the same extent within and outside the spot. On the contrary, significant differences were found in the FAA patterns of the two zones.

In order to compare data of cheese portions (i.e. spots and surrounding cheese) having different moisture contents, and considering that FAA are soluble molecules, values were expressed on the respective moisture content. Furthermore, data from both Grana Padano and Parmigiano-Reggiano were pooled to increase statistical significance. In particular, spots contained significantly higher amounts (from 4 to 12 times) of six FAA, i.e. valine ($p<0.00$), methionine ($p<0.00$), isoleucine ($p<0.00$), leucine ($p<0.00$), tyrosine ($p<0.00$) and phenylalanine ($p<0.00$) (Figure 6). It is worthy of remark that the content of the other FAA was the same as in the cheese portion around the spot. Nevertheless, this last portion had the usual FAA pattern we observed for the two target cheeses in previous studies (Cattaneo et al., 2008; Masotti et al., 2010). To achieve direct confirmation of such a different composition in individual FAA within the cheese, a simple experiment was carried out. A water solution having the approximate concentration of FAA in cheese water phase was injected into a spot-free cheese slice. After a resting time suitable to allow diffusion of the solution, the cheese was sampled taking three distinct portions: one circular, corresponding to the injection point (mimicking the spot), and two concentric rings around it, as shown in Figure 7 (inset). Despite of the approximate experimental conditions and sampling procedure, the obtained data confirmed that the same six FAA were retained in the zone where the mixture was injected, while the others diffused to the surrounding portions largely reaching an equilibrium (Figure 7).

Microscopic crystals.

Microscopic crystals were investigated through various microscopy techniques. Observations by fluorescence microscopy of cheese semi-thin sections, after resin embedding and staining with rhodamine B, allowed to see a huge number of microscopic crystals in bright red (Figure 8a). Confocal microscopy showed that crystals had different shapes, i.e. circular, oval or kidney-shaped, and their core was not fluorescent, indicating a different composition in respect to the peripheral zone (Figure 8b). The number of crystals ranged from 30 to 100 crystals/mm^2 in 18-20 months ripened cheeses and apparently was not different between cheese and inside spots. Crystals with the

254 same structure were detected in younger (three and six months of ripening) extra hard cheeses,
255 although in a lower amount (not shown).
256 Microscopic crystals observed by TEM showed a complex ultrastructure (Figure 8c). Three main
257 zones could be outlined: (i) a central star-shaped crystal, (ii) an intermediate zone and (iii) a
258 peripheral compact shell at the interface with the protein matrix. Figures 8d shows both the external
259 shell and the intermediate zone to be constituted by fibrils with prismatic morphology, radially
260 ordered and packed around the central crystal.
261 Confocal Raman microscopy was used to obtain information on the chemical composition since this
262 technique does not require any sample preparation. Area maps of the crystals, detected both inside
263 and outside the spot, confirmed the presence of distinct regions, as observed by TEM. Spectra of the
264 central star shaped crystal matched the calcium phosphate spectrum, dominated by the very strong
265 band at 986/cm and the medium band at 878/cm (Figure 9) that derived from the symmetric
266 stretching mode of the phosphate group (Sauer et al., 1994). The band at 1081/cm corresponded to
267 the stretching vibration (υ_3) of PO_4^{3-}, while the band at 588/cm to the P-O and O-P-O stretching and
268 bending modes (υ_4) of the same group. In calcium phosphate crystals, the minerals can be identified
269 by the position and shape of the main bands. Raman shifts and assignment for some calcium
270 phosphate minerals were studied by Koutsopoulos (2002). The Savitsky-Golay second derivative of
271 the spectra highlighted the presence of other weak bands attributable to the dibasic calcium
272 phosphate dehydrate form. No calcium phosphate was detected in other parts of the complex crystal
273 structure. In fact, in the outer zone, appearing as a dark area in the optical magnification used for
274 the Raman acquisition, spectra presented bands that arose from both free fatty acids and proteins
275 (Figure 10a). The spatial distribution of fatty acid/protein with respect the calcium phosphate within
276 the crystal area is shown in Figure 10b (in blue). It is evident that the crystal is immersed in the
277 cheese matrix. A deeper analysis of the spectra of this portion provided a major characterization of
278 the protein structure contribution. Usually, the amide I and III peaks in a protein are less sharply
279 resolved if compared with the signals of small peptides (Jenkins et al., 2005). In other words,

Raman spectral signatures of the single amino acids are retained in the peptide or protein, being largely derived from their side chain or backbone. The higher the resolution and intensity of the bands in a complex spectrum, the more probable the contribution of amino acids and/or small peptides. Thus, in the original spectrum collected from the cheese matrix around the phosphate crystal, some peculiar bands of amino acids were evident. In particular, a spectral subtraction of an unsaturated free fatty acid spectrum (considered as a background) from the original spectrum of the external region returned the profile of leucine (match higher than 60% with the pure spectrum of L-leucine) and phenylalanine (match equal to 53% with the pure spectrum of L-phenylalanine). Leucine was mainly characterized by the bands at 1237/cm due to the twisting of CH_2, and by the bands at 1187 and 1132/cm due to the rocking of NH_3^+, whilst phenylalanine showed a very intense band around 1000/cm. These results indicated that the protein component around the crystal was mainly due to these two amino acids, present in free form or in small peptides.

Other crystalline structures were randomly detected within the cheese and analysed by means of micro Raman spectroscopy. Only calcium carbonate crystals were identified so far. They appeared spheroidal in shape and translucent: the peaks at 1083, 1410, 713 and 284/cm confirmed their nature (Tlili et al., 2001) (data not shown). The presence of calcium carbonate in cheese seems to be attributable to the microbial metabolism that produces CO_2 (Gaucheron et al. 1999).

DISCUSSION

Speck characterization

By evaluating the confocal micro Raman spectrum and FAA composition of specks we obtained a tyrosine purity >95% confirming previous reports indicating the presence of this amino acid in these structures (Bottazzi et al., 1994; Tansman et al., 2015). Free tyrosine concentration increases in the whole cheese throughout the ripening process, like for all other FAA (Pellegrino et al., 1997). In our samples of Grana Padano and Parmigiano-Reggiano, free tyrosine concentration was approximately 0.8 g / 100 g of water phase (Figure 6), i.e. about ten times higher than its water solubility at room temperature (Grosse Daldrup et al., 2010). Therefore, formation of crystals

spread within the cheese would suggest that progress of proteolysis is not homogeneous in the matrix thus leading to FAA accumulation, including tyrosine, preferentially into micro openings until saturation. Furthermore, we have obtained by light microscopy further structural details of tyrosine crystals from cheese (Figure 2), showing that the former reported description (Tansman et al., 2015) is due to micro spike of the crystalized amino acid. When observed by atomic force microscopy in protein hydrolysates (McPherson et al., 2012), tyrosine crystals appeared to be covered by a stable layer of 3-nm particles, likely represented by micellar arrangement of small peptides present in the medium and able to prevent re-solubilisation of crystals once formed. Considered the remarkable content of peptides in ripened cheeses, this aspect would be worthy of investigation.

Spot characterization

Contrary to the hard specks, spots were easily resin embedded and cut into thin sections that allowed a deeper characterization by various microscopy techniques. Previous studies on spots in cheese did not investigate their structure and ultrastructure (Giolitti and Mascherpa, 1970; Bianchi et al. 1974; Tansman et al., 2015). Unexpectedly, when the cheese was directly stained with ninhydrin and observed by light microscopy, the original grains of curd were still visible. During cheese manufacturing, curd grains (20-50 mm), obtained by cutting the rennet gel, are let in hot whey for 50-60 min to settle and aggregate at the bottom of the vat. Further fusing and shrinking of curd grains are induced by the subsequent acidification of the cheese loaf when kept in mould for 48 hours. Since Grana Padano and Parmigiano-Reggiano loaves are not pressed, high temperature and low pH (5.2-5.3) play the major role in promoting whey draining (Pellegrino et al., 1997) and the tight aggregation of curd grains. However, as said above, these grains appeared as separate units even several months later. The junctions between contiguous grains are low in fat because many fat globules escape the protein network at the surface of the grains before they stick together. For those grains having either irregular shape or different size their aggregation during settling forms an internal hole, connected with several openings and radial junctions. This pattern was frequently

observed within the spots (Figure 3b). In the young cheese, even before the spot formation, these hollow cavities likely represent preferential zones where whey stagnates and entrapped bacterial cells find substrates for growth (Le Boucher et al., 2016). Growth of bacterial colonies as affected by local concentration of substrates in cheese is receiving increasing attention (Silva et al., 2013; Jeanson et al., 2015). Although no intact bacterial cells were detected by TEM in cavities within the spot, as well as in the surrounding cheese, likely due to the prolonged ripening process, an indirect, preliminary confirmation of this hypothesis came out by measuring the amount of total DNA extracted from the spot and the surrounding cheese following the procedure of (Cremonesi et al., 2007). In fact, DNA amount was more than three times higher in the spots than in the surrounding cheese (72.94 µg *vs* 22.41 µg/mg).

Spots proved to be significantly more dry, with respect to the surrounding cheese portion, and to contain more protein and less ash (Table 1), confirming the data reported by Tansman et al. (2015). In addition, we showed the cheese portion just around the spot had the same chemical composition as the rest of the cheese, confirming that the spot is a fully isolated unit. The dense layer we observed around it by light microscopy is likely responsible for this (Figure 3, arrowhead). Overall, these findings point to a migration of whey, with consequent draining of solutes, occurring locally within the cheese where the spot would originate later.

Spots were also reported to have a different FAA composition compared to the whole cheese. Bianchi et al. (1974) found spots in 18- and 25-month ripened Grana Padano cheeses to contain (g/100 g): leucine (9.86), isoleucine (4.96), methionine (1.64), valine (1.52), glutamic acid (1.84), and asparagine (1.63), as dominant FAA. However, these authors did not notice that the last two FAA were equally abundant in the whole cheese. Recently, Tansman et al. (2015) detected only 1% of free leucine in spots from a 24-month old Parmigiano-Reggiano cheese but they did not give explanation for the discrepancy of this result with those of literature. We obtained FAA data similar to those of Bianchi et al. (1974), however we put forward a different interpretation. The key to understand the genesis of the spot relays in the chemical properties of the different FAA present in

the spot and in the cheese regardless of their concentration. In fact, the six FAA we detected at much higher levels in the spot (i.e. leucine, isoleucine, methionine, valine, phenylalanine and tyrosine) (Figure 6) are all hydrophobic because of either the aromatic or branched chain structure, and thus insoluble in the water phase of cheese. This shared FAA characteristic leads us to hypothesise that local water movements are responsible for their different distribution and, consequently, for the spot blowing in hard and extra hard cheeses. This hypothesis was confirmed by our experiment mimicking the migration of FAA within the cheese.

As already mentioned, in young cheese the cavities in which the residual whey stagnates could be the sites where bacterial colonies develop. During cheese ripening, the water phase in these sites becomes more concentrated in solutes due to lactic acid bacteria metabolism and, at a later stage, to cell lysis. Progressively, the water phase migrates through the curd grain junctions, dragging solutes including, preferentially, polar FAA over the hydrophobic ones. Consequently, less water soluble molecules concentrate in a restricted area, that evolves into a spot, from which water moves away radially (Figure 7) dragging away also salts. For this reason, many crystals were visible in the junctions (Figure 4c).

Microscopic crystal characterization

Microcrystals appeared to be spread within the whole cheese. Among these crystals we have up to now identified calcium phosphate by micro Raman, directly on the cheese, without any sample preparation. The central star shaped crystals observed by TEM (Figure 8c) were clearly assigned to selected types of calcium phosphate. Gaucheron et al. (1999) demonstrated that the supersaturation of calcium phosphate salts increases strongly during cheese ripening due to the rise of pH, explaining the salt precipitation. Unfortunately, the few references that discuss crystals ultrastructure in cheese give no indication about the nature of the calcium phosphate. In our study, the micro Raman analysis produced sufficient information about their morphological features and complex ultrastructure. In fact, this technique allowed to evidence for the first time that the fibrillary layer surrounding the central crystal contains leucine and, to a lower amount,

phenylalanine. These hydrophobic amino acids are reported to limit growth of calcium phosphate crystals due to their absorption on the crystal surface that blocks the active growth sites (Dalas et al., 2008). Although calcium lactate could form in cheese, due to lactic acid fermentation, the chelation of calcium by the phosphates should greatly prevail (Heertje et al., 1981), in agreement with the relevant number of calcium phosphate crystals we detected. Arkwall et al. (2006) reported that calcium lactate crystals only form when pH is higher than 5.1. We could not find calcium lactate crystals, although we cannot exclude their presence in extra hard cheeses, as different unidentified crystalline structures were observed by TEM. Some researcher detected calcium lactate crystals in cheeses other than Grana Padano and Parmigiano-Reggiano (Washam et al., 1982; Tansman et al., 2014), whereas only Bottazzi et al. (1982) detected them in 14-month ripened Grana cheese indicating their low incidence, i.e. 2-3 per square mm.

Presence of leucine crystals is likely within the spot where free leucine showed a concentration in the water phase ten times higher than in the cheese (Figure 6). Crystalline leucine was also detected by Tansman et al. (2015) in pearls collected from Parmigiano-Reggiano cheese.

CONCLUSIONS

In conclusion, combining the background knowledge about extra-hard cheese manufacturing and ripening with the new information about composition and structure of spots achieved in this study, we can hypothesize an incomplete aggregation of curd granules and a consequent local whey stagnation to be at the origin of spot development. Growth and lysis of bacterial cells entrapped in these micro cavities influence both metabolite availability and micro environmental conditions, that in turn regulate diffusion and crystallization of solutes locally. Therefore, all practices finalized to the syneresis improvement, such as fine-tuning of temperature control and curd grain size, would greatly reduce spot number and the occurrence of other confined phenomena.

REFERENCES

Agarwal, S., J. R. Powers, B. G. Swanson, S. Chen, and S. Clark. 2006. Cheese pH, protein concentration, and formation of calcium lactate crystals. J. Dairy Sci. 89: 4144-4155.

Agarwal, S., K. Sharma, B. G. Swanson, G. U. Yüksel, and S. Clark. 2006. Nonstarter lactic acid bacteria biofilms and calcium lactate crystals in Cheddar cheese. J. Dairy Sci. 89: 1452–1466.

Babcock, S. M., L. H. Russel, A. Vivian, and U. S. Baer. 1903. Condition affecting the development of white specks in cold-curd cheese. Pages 180-183 in Wis. Agric. Expt. Sta. 19th Annu. Rep.

Bianchi, A.; G. Beretta, G. Caserio, and G. Giolitti. 1974. Amino acid composition of granules and spots in Grana Padano cheeses. J. Dairy Sci. 57: 1504–1508.

Bottazzi, V., B. Battistotti, and F. Bianchi. 1982. The microscopic crystalline inclusions in Grana cheese and their x-ray microanalysis. Milchwissenschaft Milk Sci. Internat. 37: 577–580.

Bottazzi, V., F. Lucchini, A. Rebecchi, and G. L. Scolari. 1994. I cristalli del formaggio grana (Crystals present in Grana cheese). Sci. Tecn. Latt.-Cas. 45: 7–14.

Cattaneo, S., J. A. Hogenboom, F. Masotti, V. Rosi, L. Pellegrino, and P. Resmini. 2008. Grated Grana Padano cheese: new hints on how to control quality and recognize imitations. Dairy Sci. Technol. 88: 595-605.

Codex General Standard for Cheese. Codex Standard 283-1978.

Cremonesi, P., G. Perez, G. Pisoni, P. Moroni, S. Morandi, M. Luzzana, M. Brasca, and B. Castiglioni. 2007. Detection of enterotoxigenic Staphylococcus aureus isolates in raw milk cheese. Lett. Appl. Microbiol. 45: 586–591.

Culka, A., J. Jehlicka, and H. G. M. Edwards. 2010. Acquisition of Raman spectra of amino acids using portable instruments: Outdoor measurements and comparison. Spectrochim. Acta A. 77: 978–983.

Dalas, E., P. Malkaj, Z. Vasileiou, and D. G. Kanellopoulou. 2008. The effect of Leucine on the crystal growth of calcium phosphate. J. Mater. Sci.: Mater. Med. 19: 277-282.

D'Incecco, P., F. Faoro, T. Silvetti, K. Schrader, and L. Pellegrino. 2015. Mechanisms of Clostridium tyrobutyricum removal through natural creaming of milk: A microscopy study. J. Dairy Sci. 98: 5164-5172.

Gatti, M., B. Bottari, C. Lazzi, E. Neviani, and G. Mucchetti. 2014. Invited review: Microbial evolution in raw-milk, long-ripened cheeses produced using undefined natural whey starters. J. Dairy Sci. 97: 573-591.

453 Gaucheron, F., Y. Le Graet, F. Michel, V. Briard and M. Piot. Evolution of various salt
454 concentrations in the moisture and in the outer layer and centre of a model cheese during its
455 brining and storage in ammoniacal atmosphere. Lait. 79: 553-566.

456

457 Giolitti, G. and G. F. Mascherpa. 1970. La formazione di depositi di tirosina in formaggi a lunga
458 stagionatura. Ind. Latte. 6: 83-85.

459

460 Grosse Daldrup, J. B., C. Held, F. Ruether, G. Schembecker, and G. Sadowski. 2009. Measurement
461 and modeling solubility of aqueous multisolute amino-acid solutions. Ind. Eng. Chem. 49:
462 1395–1401.

463

464 Heertje, I., M. J. Boskamp, F. Van Kleef, and F. H. Gortemaker. 1981. The microstructure of
465 processed cheese. Neth. Milk Dairy J. 35, 177.

466

467 Jeanson, S., J. Floury, V. Gagnaire, S. Lortal, and A. Thierry. 2015. Bacterial colonies in solid
468 media and foods: a review on their growth and interactions with the micro-environment.
469 Front. Microbiol. 6: 1284.

470

471 Jenkins, A. L., R. A. Larsen, and T. B. Williams. 2005. Characterization of amino acids using
472 Raman spectroscopy. Spectrochim. Acta A. 61: 1585–1594.

473

474 Kaláb, M., J. Yun, and S. H. Yiu. 1987. Textural properties and microstructure of process cheese
475 food rework. Food Microbiol. 6: 181-192.

Koutsopoulos, S. 2002. Synthesis and characterization of hydroxyapatite crystals: a review study on the analytical methods. J. Biomed. Mater. Res., 62: 600-612.

Le Boucher, C., V. Gagnaire, V. Briard-Bion, J. Jardin, M. B. Maillard, G. Dervilly-Pinel, B. Le Bizec, S. Lortal, S. Jeanson, and A. Thierry. 2016. Spatial distribution of Lactococcus lactis colonies modulates the production of major metabolites during the ripening of a model cheese. Appl. Environ Microbiol. 82: 202–210.

Marcos, A. 1993. Water activity in cheese in relation to composition, stability and safety. Pages 439-469 in Cheese: Chemistry, Physics and Microbiology, Vol. 1, ed.; Fox. P. F.; Chapman & Hall, London.

Masotti, F., J. A. Hogenboom, V. Rosi, I. De Noni, and L. Pellegrino. 2010. Proteolysis indices related to cheese ripening and typicalness in PDO Grana Padano cheese. Int. Dairy J. 20: 352-359.

McPherson, A., S. B. Larson, and Y. G. Kuznetsov. 2012. Tyrosine Microcrystals Produced by Digestion of Proteins with Pancreatic Enzymes. Crystal Growth & Design. 12: 3594-3602.

McSweeney, P. L. H. 2004. Biochemistry of cheese ripening. Int. J. Dairy Technol. 57:127–144.

Ong, L., R. R. Dagastine, S. E. Kentish, and S. L. Gras. 2010. Transmission electron microscopy imaging of the microstructure of milk in cheddar cheese production under different processing conditions. J. Food Sci. 75: 135–145.

Pellegrino, L. G. Battelli, P. Resmini, P. Ferranti, F. Barone, and F. Addeo. 1997. Effects of heat load gradient occurring in moulding on characterization and ripening of Grana Padano. Lait. 77: 217-228.

Sauer, G. R., W. B. Zunic, J. R. Durig, and R. E. Wuthier. 1994. Fourier transform Raman spectroscopy of synthetic and biological calcium phosphates. Calcif. Tissue Int. 54: 414-420.

Schrader, K. 2012. Structural analysis of milk and milk products. Strukturanalyse von Milch und Milchprodukten. 133: 30-34.

Shock, A. A., W. J. Harper, A. M. Swanson, and H. H. Sommer. 1948. What's in those "white specks" on Cheddar. Wisconsin Agric. Experiment. Station. Bull. 474: 31–32.

Silva, J. V. C., P. D. S. Peixoto, S. Lortal, and J. Floury. 2013. Transport phenomena in a model cheese: the influence of the charge and shape of solutes on diffusion. J. Dairy Sci. 96: 6186–6198.

Tansman, G., P. S. Kindstedt, and J. M. Hughes. 2014. Powder x-ray diffraction can differentiate between enantiomeric variants of calcium lactate pentahydrate crystal in cheese. J. Dairy Sci. 97: 7354–7362.

Tansman, G., P. S. Kindstedt, and J. M. Hughes. 2015. Crystal fingerprinting: elucidating the crystals of Cheddar, Parmigiano-Reggiano, Gouda, and soft washed-rind cheeses using powder x-ray diffractometry. Dairy Sci. Technol. 95: 651–664.

Tlili, M. M., M. Ben Amor, C. Gabrielli, S. Joiret, G. Maurin, and P. Rousseau. 2001. Characterization of CaCO3 hydrates by micro-Raman Spectroscopy. J. Raman Spectrosc. 33. 10–16.

Tuckey, S. L., H. A. Ruehe, and G. L. Clark. 1938. X-ray diffraction analysis of white specks in Cheddar cheese. J. Dairy Sci. 21: 161.

Washam, C. J., T. J. Kerr, V. J. Hurst, and W. E. Rigsby. 1985. A scanning electron microscopy study of crystalline structures on commercial cheese. Dev. Ind. Microbiol. 26: 749–761.

537 **TABLES**

538 **Table 1**. **Chemical composition of spot, cheese portion around it and whole cheese.***

	MOISTURE	FAT	PROTEIN	ASH
SPOT	$24.2^{a} \pm 1.2$	$27.5^{a} \pm 2.6$	$37.6^{a} \pm 1.3$	$3.9^{a} \pm 0.1$
CHEESE AROUND THE SPOT	$29.5^{b} \pm 1.0$	$29.6^{a} \pm 1.2$	$33.5^{b} \pm 0.6$	$4.4^{b} \pm 0.3$
WHOLE CHEESE	$29.8^{b} \pm 1.0$	$29.9^{a} \pm 1.1$	$33.5^{b} \pm 0.2$	$4.4^{b} \pm 0.2$

539

540 * Data were mean ± standard deviation based on duplicate analyses of five cheeses.

541 [a, b] Means in the same column with different letters are significantly different (p= 0.05).

542

FIGURE CAPTIONS

Figure 1. Photograph of extra hard cheese showing speaks (SK) and spots (ST). (CS) cheese portion surrounding a spot, sampling mode. Inset, isolated spots from the cheese.

Figure 2. Free amino acid analysis and (inset) light microscopy of a speck isolated from cheese. Bar=200 µm.

Figure 3. Hand-made section of Grana Padano cheese including a spot: light microscopy after ninhydrin staining revealed a dense layer limiting the spot (arrowhead) and the junctions among curd granules (arrows). Bar=200 µm.

Figure 4. Light microscopy of spot semi-thin section (2-5µm) stained with toluidine blue. (a) the curd junctions are visible as darker lines; bar=200 µm. (b): Detail of the large hole in which junctions converge; bar=50 µm. (c) Microcrystals (arrows) along a curd junction; bar=10 µm.

Figure 5. Ultrathin section of spot ultrastructure (a) in comparison with the surrounding cheese (b): the network of electron dense proteins shows a more irregular profile in the spot, particularly at the interface with the electron transparent fat matrix; bar=1 µm.

Figure 6. Free amino acid content of the spot and the cheese portion around it. Data were mean of duplicate analyses of eleven cheeses. (*) Values statistically different ($p<0.05$).

565 **Figure 7**. Free amino acid content of the portions 1-3 taken from cheese after the diffusion of 0.3
566 mL aqueous amino acid solution injected in 1 (inset). Data were mean of duplicate analyses.

567

568 **Figure 8.** Calcium phosphate crystals in cheese. (a) Fluorescence microscopy of crystals stained
569 with rodhamine B. (b) Video confocal microscopy of crystals stained with fast green and observed
570 with TRITC and FITC filters, revealing a non-fluorescent core. (c) Ultrathin section of a crystal
571 showing a star shaped zone in the center; at the interface with protein matrix, the fibrillar structure
572 of the crystal is visible (d).

573

574 **Figure 9.** Raman spectrum of calcium phosphate crystal in cheese. Stars represent typical signals of
575 the salt.

576

577 **Figure 10.** Raman spectra (a) and images (b) of spatial distribution of lipid/protein components
578 (red/green areas) around the crystal (covered by the blue area). High, medium and very low
579 component concentrations are indicated as red, green and blue respectively.

580

FIGURE CAPTIONS (printed and on-line version)

Figure 1. Photograph of extra hard cheese showing speaks (SK) and spots (ST). (CS) cheese portion surrounding a spot, sampling mode. Inset, isolated spots from the cheese.

Figure 2. Free amino acid analysis and (inset) light microscopy of a speck isolated from cheese. Bar=200 µm.

Figure 3. Hand-made section of Grana Padano cheese including a spot: light microscopy after ninhydrin staining revealed a dense layer limiting the spot (arrowhead) and the junctions among curd granules (arrows). Bar=200 µm.

Figure 4. Light microscopy of spot semi-thin section (2-5µm) stained with toluidine blue. (a) the curd junctions are visible as darker lines; bar=200 µm. (b): Detail of the large hole in which junctions converge; bar=50 µm. (c) Microcrystals (arrows) along a curd junction; bar=10 µm.

Figure 5. Ultrathin section of spot ultrastructure (a) in comparison with the surrounding cheese (b): the network of electron dense (grey) proteins shows a more irregular profile in the spot, particularly at the interface with the electron transparent (white) fat matrix; bar=1 µm.

Figure 6. Free amino acid content of the spot and the cheese portion around it. Data were mean of duplicate analyses of eleven cheeses. (*) Values statistically different ($p<0.05$).

Figure 7. Free amino acid content of the portions 1-3 taken from cheese after the diffusion of 0.3 mL aqueous amino acid solution injected in 1 (inset). Data were mean of duplicate analyses.

Figure 8. Calcium phosphate crystals in cheese. (a) Fluorescence microscopy of crystals stained with rodhamine B. (b) Video confocal microscopy of crystals stained with fast green and observed with TRITC and FITC filters, revealing a non-fluorescent core. (c) Ultrathin section of a crystal showing a star shaped zone in the center; at the interface with protein matrix, the fibrillar structure of the crystal is visible (d).

Figure 9. Raman spectrum of calcium phosphate crystal in cheese. Stars represent typical signals of the salt.

Figure 10. Raman spectra (a) and images (b) of spatial distribution of lipid/protein components around the crystal (central dark grey area).

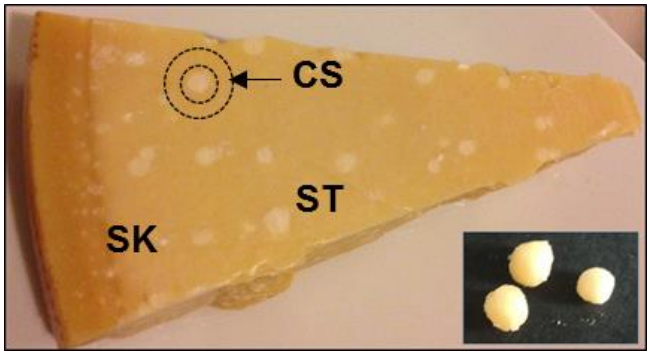

D'Incecco Figure 1.

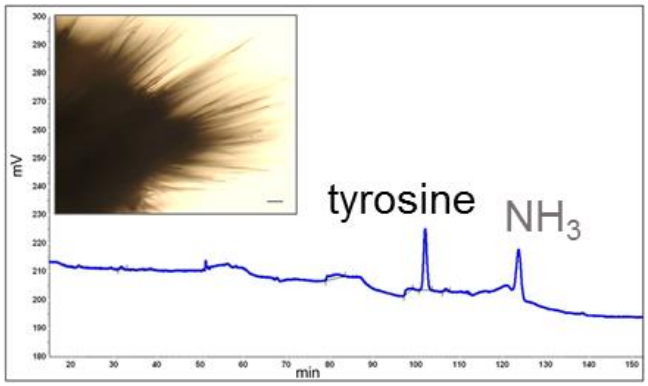

D'Incecco Figure 2.

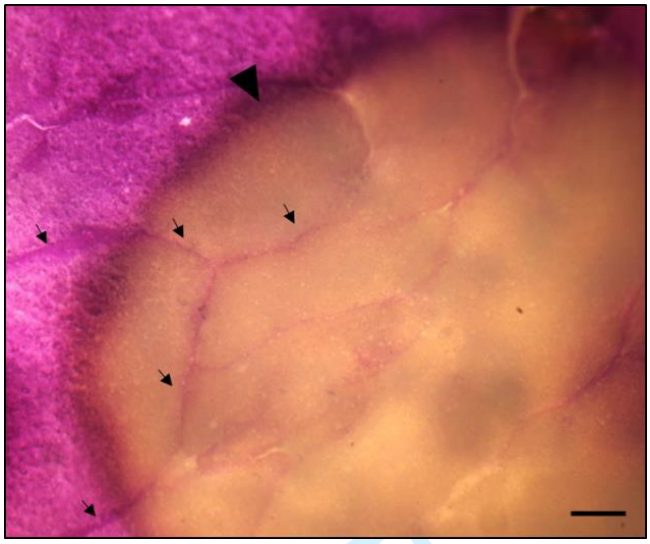

D'Incecco Figure 3.

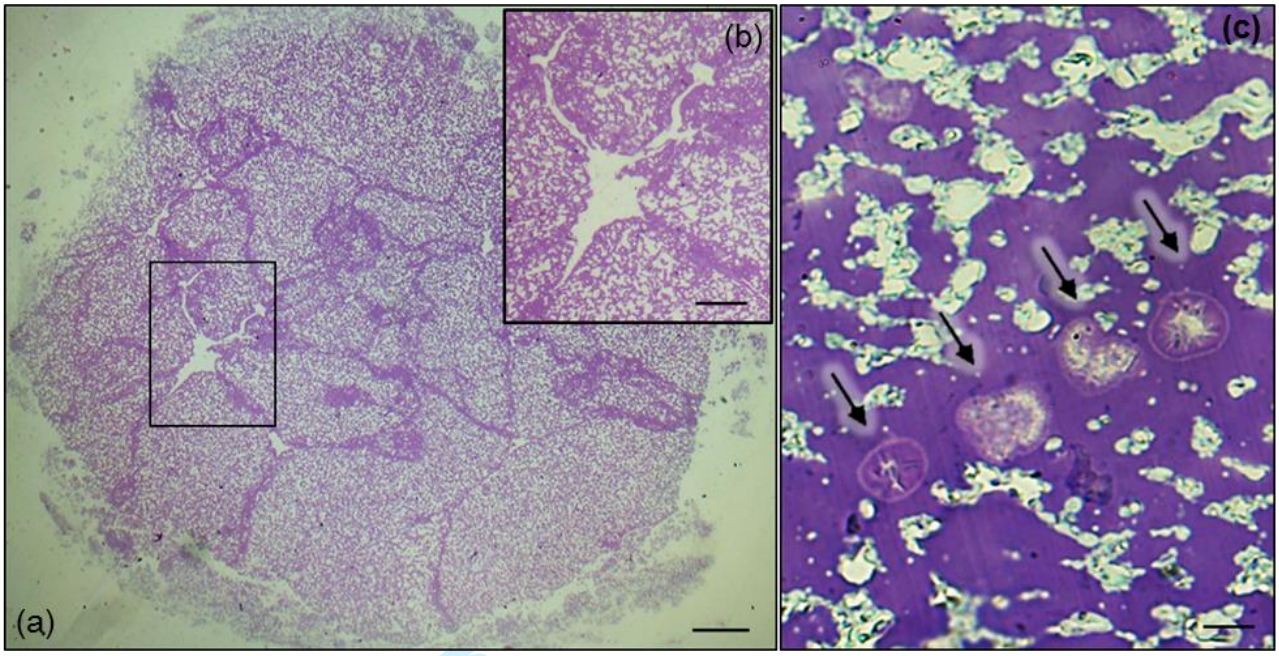

D'Incecco Figure 4.

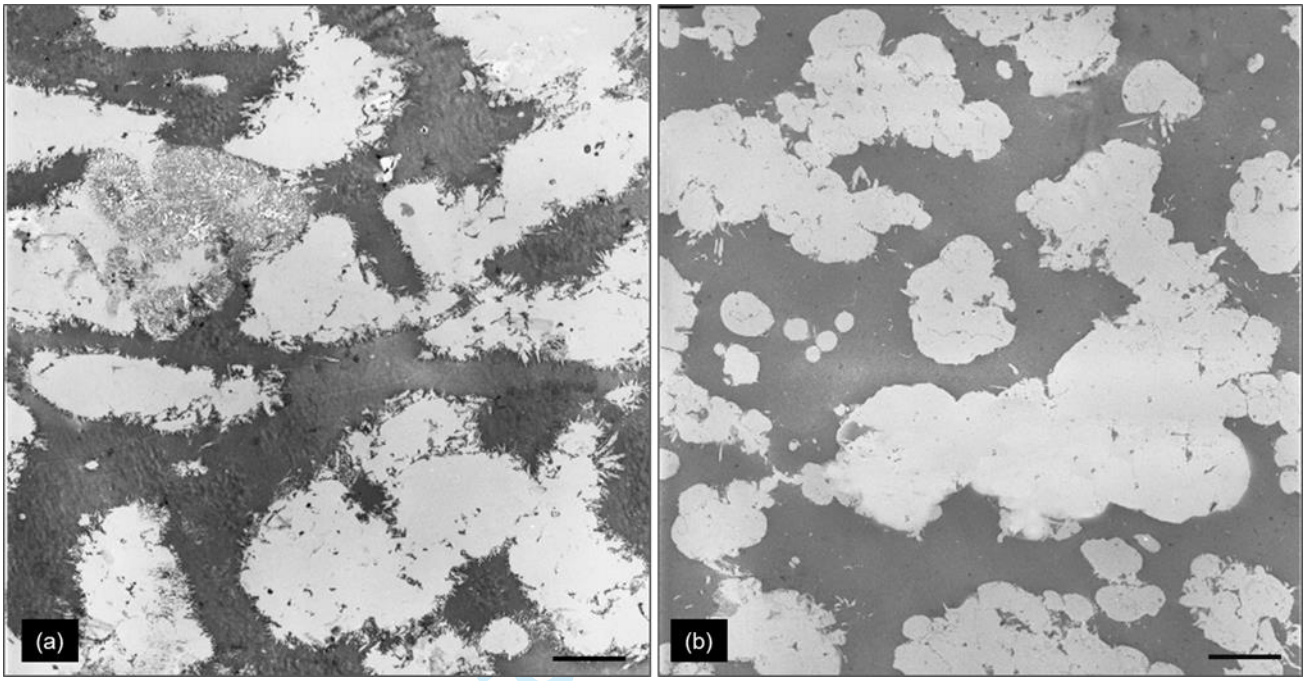

D'Incecco Figure 5.

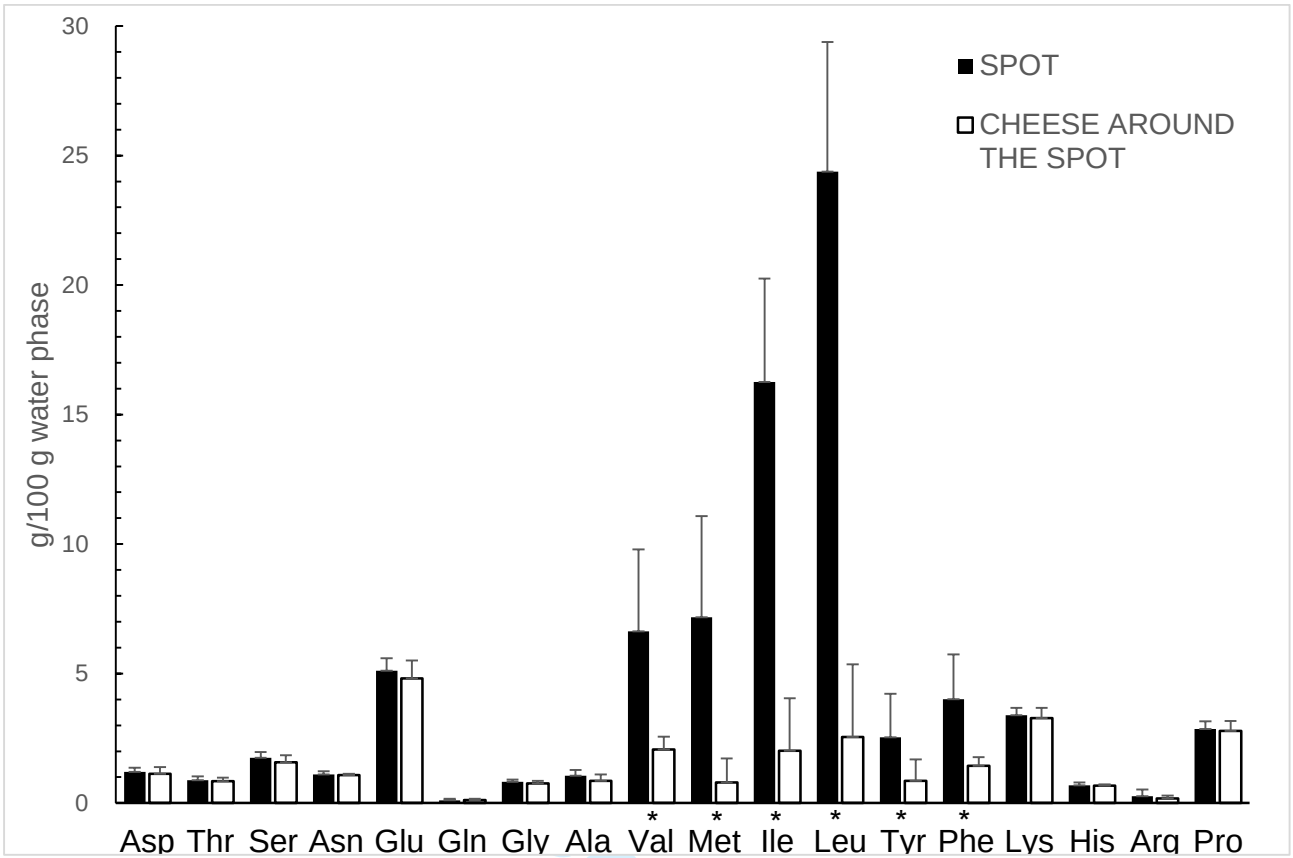

D'Incecco Figure 6.

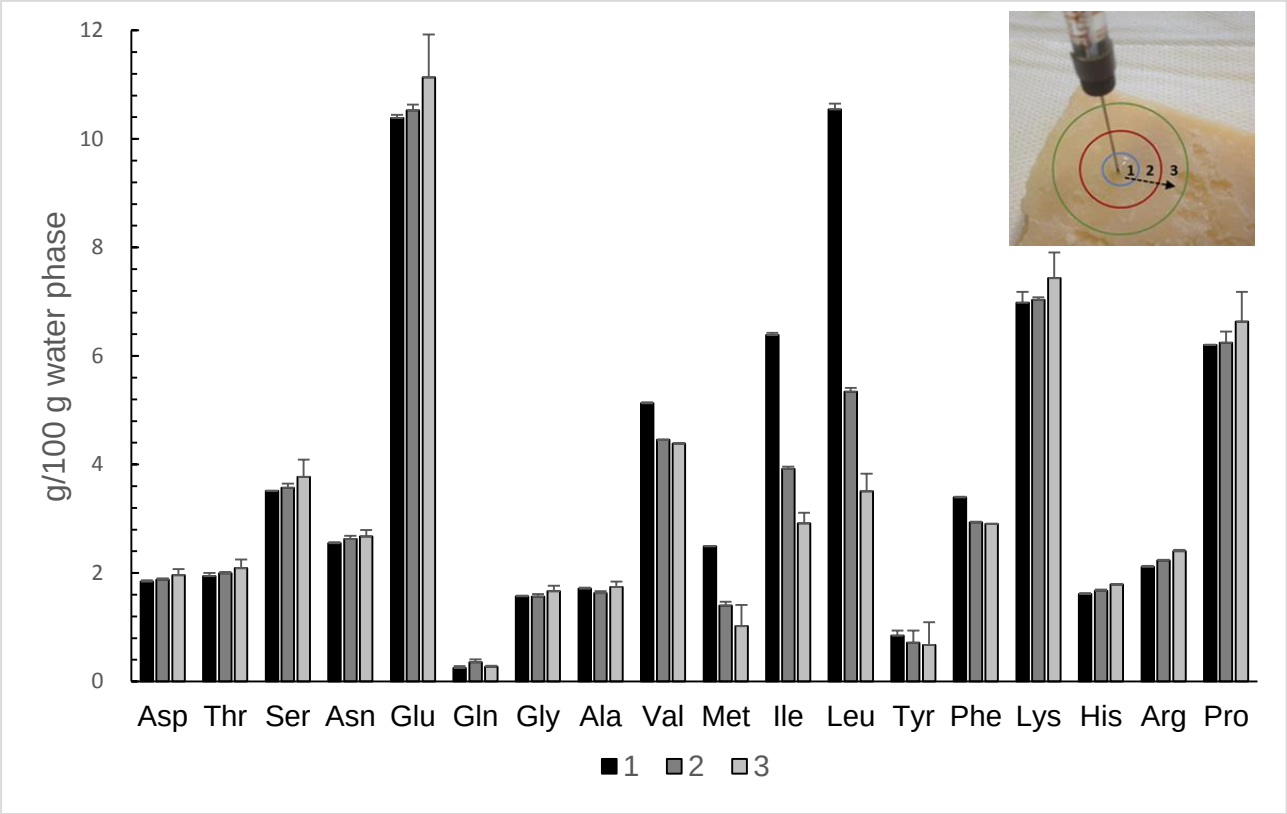

D'Incecco Figure 7.

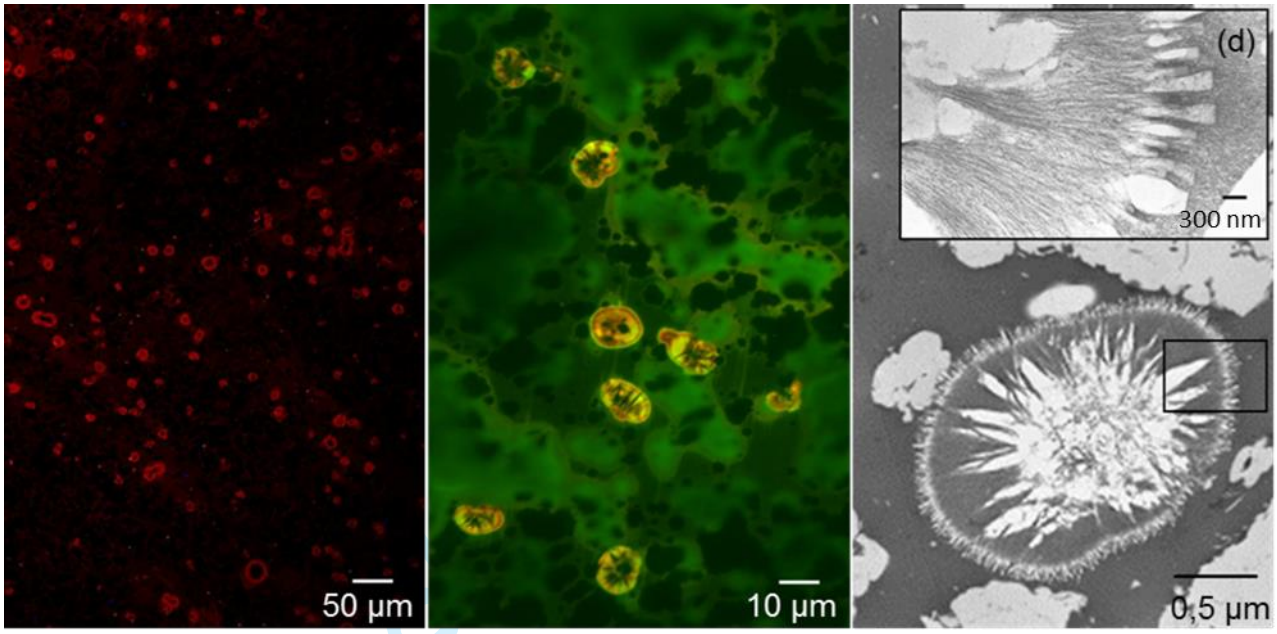

D'Incecco Figure 8.

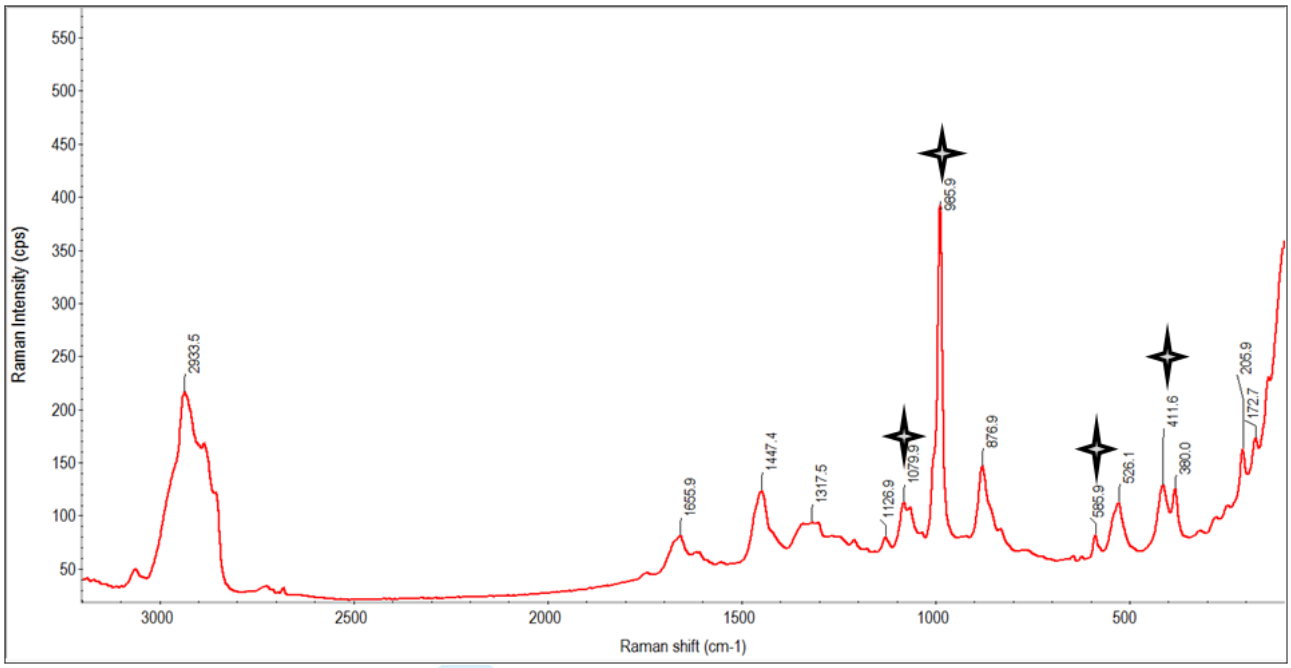

D'Incecco Figure 9.

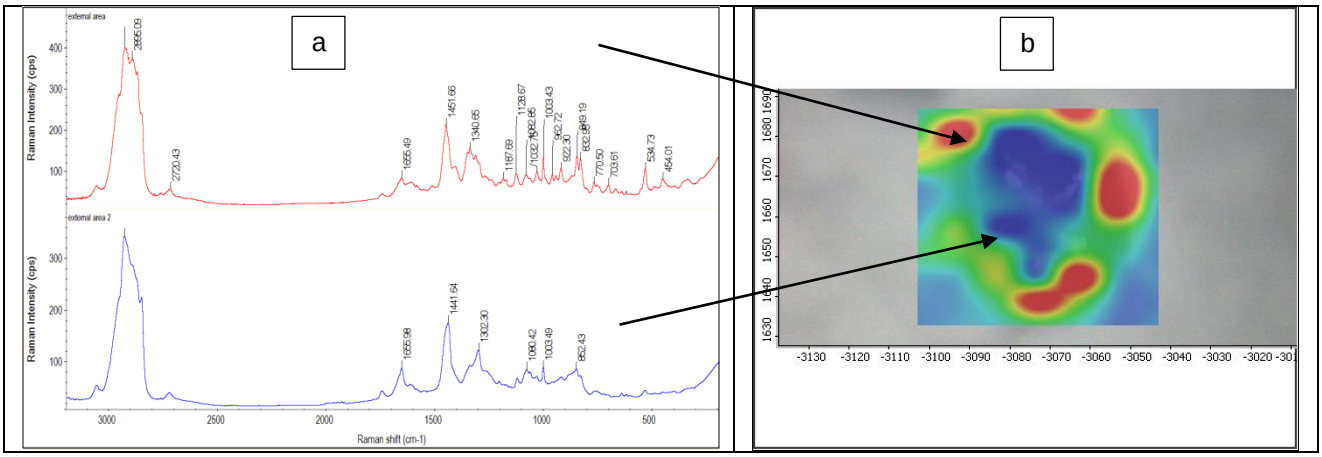

D'Incecco Figure 10.